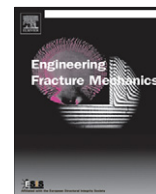




ELSEVIER

Contents lists available at ScienceDirect

Engineering Fracture Mechanics

journal homepage: www.elsevier.com/locate/engfracmech

Fatigue limit prediction of notched components using short crack growth theory and an asymptotic interpolation method

Yongming Liu ^{a,*}, Sankaran Mahadevan ^b^a Clarkson University, Potsdam, NY 13699, USA^b Vanderbilt University, Nashville, TN 37235, USA

ARTICLE INFO

Article history:

Received 16 December 2007

Received in revised form 18 June 2008

Accepted 19 June 2008

Available online xxxx

Keywords:

Notch

Fatigue

Life prediction

Asymptotic solution

ABSTRACT

Mechanical components have stress risers, such as notches, corners, welding toes and holes. These geometries cause stress concentrations in the component and reduce the fatigue strength and life of the structure. Fatigue crack usually initiates at and propagates from these locations. Traditional fatigue analysis of notched specimens is done using an empirical formula and a fitted fatigue notch factor, which is experimentally expensive and lacks physical meaning. A general methodology for fatigue limit prediction of notched specimens is proposed in this paper. First, an asymptotic interpolation method is proposed to estimate the stress intensity factor (SIF) for cracks at the notch root. Both edge notched and center notched components with finite dimension correction are included into the proposed method. The small crack correction is included in the proposed asymptotic solution using El Haddad's fictitious crack length. Fatigue limit of the notched specimen is estimated using the proposed stress intensity factor solution when the realistic crack length is approaching zero. A wide range of experimental data are collected and used to validate the proposed methodology. The relationship between the proposed methodology and the traditionally used fatigue notch factor approach is discussed.

© 2008 Elsevier Ltd. All rights reserved.

1. Introduction

The stress concentration effect on fatigue life predictions of mechanical components is an important issue in fatigue reliability evaluation. The problem has been investigated in many studies but still has not been fully solved. Different approaches have been proposed to include the effects of notch and stress concentrations. These approaches can be grouped into several categories. One approach is the so called theory of critical distance (TCD) [1]. A detailed review of this approach and its similar variations can be found in [2]. Another approach is based on the stress gradient formulation for the fatigue analysis of notched components [3]. The cohesive zone model (CZM) is another important methodology for fatigue analysis of notched specimens [4]. However, the application seems to be mostly for composite and concrete materials, which show brittle and/or quasi-brittle behavior [5,6]. A comprehensive review of the fatigue analysis approaches for notched specimens is not the focus of this paper. Only two of them, which are dominantly used in the research community and industry, are discussed below. One is based on the classical fatigue theory, i.e. $S-N$ curve-based approach. The other is the fracture mechanics-based approach, i.e. $da/dN \sim \Delta K$ curve-based crack growth analysis.

* Corresponding author. Tel.: +1 315 268 2341; fax: +1 315 268 7985.

E-mail address: yliu@clarkson.edu (Y. Liu).

1.1. Classical S–N curve-based approaches

For classical fatigue analysis, a knock down factor is usually introduced to consider the detrimental effect of stress concentration on the material S–N curve [7]. Earlier methods used a fatigue notch factor K_f defined as [8]

$$K_f = \frac{\text{unnotched fatigue strength}}{\text{notched fatigue strength}} \quad (1)$$

Several methods of fatigue notch factor calculation have been proposed. Peterson [9] proposed the formula

$$q = \frac{K_f - 1}{K_t - 1} = \frac{1}{1 + \frac{C_p}{\rho}} \quad (2)$$

where K_t is the elastic stress concentration factor, ρ is the notch tip radius, C_p is a material parameter related to the ultimate tensile strength. Neuber [10] proposed a similar formula with a different exponent of ρ as

$$q = \frac{K_f - 1}{K_t - 1} = \frac{1}{1 + \sqrt{\frac{C_N}{\rho}}} \quad (3)$$

where C_N is a material parameter. A different weight factor considering the notch radius effect was proposed by Heywood [11] as

$$q = \frac{K_f - 1}{K_t - 1} = \frac{1}{1 + 2\sqrt{\frac{C_H}{\rho}}} \quad (4)$$

There are many other models with similar formulas as discussed above. Those models are not listed here and can be found in a previous review paper [12]. The basic idea of this type of approach is to assume that the fatigue strength of notch specimen is controlled by the stress at a specific location or averaged over a domain from the notch tip. This assumption lacks physical foundation, and is thus empirical in nature. The material parameters used in this approach need to be calibrated using extensive experimental results of various notched specimens with different notch geometries.

As reviewed by Ciavarella and Meneghetti [7], one of the major limitations of the fatigue notch factor is that it is not applicable to very sharp notches. For example, Peterson's formula can be rewritten as Eq. (5) for very sharp notches (small ρ).

$$K_f = 1 + (K_t - 1) \frac{\rho}{C_p} \quad (5)$$

Eq. (5) implies that K_f approaches unity when the tip radius is very small regardless of the notch depth. This is obviously not correct since a very sharp notch can be treated as a crack if the notch is sufficiently deep and it will lead to the lower fatigue strength of the specimen. The notch factor K_f should not be unity according to Eq. (1). Other formulas have the same limitation as they also predict that the fatigue notch factor is unity for sharp notches.

1.2. Fracture mechanics-based approaches

The application of fracture mechanics for fatigue analysis has been very successful in the past decades, especially for damage tolerance design of components having crack-like defects or geometries. The key assumption of fracture mechanics-based fatigue analysis is that the fatigue process is actually a crack growth process. Compared to the classical S–N curve-based approach for fatigue analysis, there is no empirical "fatigue damage" quantity in the fracture mechanics-based approach. The crack growth process can be predicted using a fracture mechanics-based driving force parameter (i.e., stress intensity factor or J integral) and a material crack growth rate curve.

A straightforward way to include the notch effect is to use the stress intensity factor solution of a crack at the notch tip. A classical solution of the elastic stress field ahead of the notch tip was proposed by Creager and Paris [13] as

$$\sigma_{yy} = \frac{K}{\sqrt{2\pi x}} \left(1 + \frac{\rho}{2x}\right) \quad (6)$$

where x is the coordinate along the horizontal axis, and K is the stress intensity factor. The origin of the coordinate system is located at $\frac{\rho}{2}$ behind the notch tip. Many other analytical and numerical solutions have been proposed in the literature and handbooks for stress field solution of notches. Kujawski [14] proposed a stress intensity factor formula for short cracks at a notch as

$$\Delta K = 1.122 \frac{K_t \Delta \sigma}{2} \left[\left(1 + 2\frac{a}{\rho}\right)^{-1/2} + \left(1 + 2\frac{a}{\rho}\right)^{-3/2} \right] \sqrt{\pi a} \quad (7)$$

where K_t is the stress concentration factor, $\Delta \sigma$ is the applied stress range, a is the crack length.

Jones et al. [15] proposed an equation for a semi-elliptical crack at a notch as

$$K_I(\phi) = \left\{ \frac{\sigma}{E(K)} \sqrt{\pi a} (\sin^2 \phi + (c/a)^2 \cos^2 \phi)^{1/4} \right\} F \quad (8)$$

where a is the depth and $2c$ is the surface length of a semi-elliptical flaw. The parameter ϕ is the angle in the parametric equation of ellipse and $E(k)$ is complete integral of the second kind. F is a correction factor considering the notch radius and boundary conditions. F can be expressed as

$$F = F_e + (F_s - F_e) e^{-a_\phi/\rho} \quad (9)$$

where F_e and F_s are the boundary correction factors for an embedded crack, and a surface crack in a plate, respectively, and were taken from Newman et al. [16].

Once a stress intensity factor (SIF) solution is obtained, fatigue life can be predicted using material fatigue crack growth (FCG) properties. Locke et al. [17] used the SIF solution given by Chell [18] and predicted the crack growth rate of Wasply specimens with different notch depth and radius. Ahmad et al. [19] used strain field solution ahead of the notch tip and FCG properties expressed using strain range to predict fatigue life. This approach assumes two stages of crack growth, i.e. small crack growth and long crack growth. The initial crack size for small crack growth is taken as 0.5 μm . Dabayeh et al. [20] used a strain intensity factor solution obtained from finite element analysis for life prediction. The initial crack length is assumed to be 3 μm . Hammouda et al. [21] used the stress intensity solution of Cameron and Smith [22] to predict the crack growth rate of low carbon steel. The FCG is in the Paris regime and the initial crack length is around 0.1 mm. Newman et al. [23] used FASTRAN software to predict fatigue life of notched steel and aluminum alloy specimens. Small crack growth theory is used and the initial crack length is set to be around 10–20 μm . Medved et al. [24] used AFGROW software to calculate the crack growth life from corrosion pits at the notch tip. The initial crack size is estimated based on the back-extrapolation method and the FCG is in the Paris regime. There are a few other studies also focused on the crack growth analysis of notch specimen and are not discussed here [25,26].

From the brief discussion above, it is found that, compared with a large number of studies using the classical $S-N$ curve-based approach modified using the fatigue notch factor, the fracture mechanics-based approach has not been fully explored. The classical notch fatigue analysis (i.e., $S-N$ curve-based) can predict the notch fatigue behavior but requires extensive experimental calibration. Fracture mechanics-based approaches can be used to explain the notch fatigue behavior based on a sound physical argument. However, there is no universally accepted method for fatigue crack growth from a notch, especially considering both near threshold short crack and Paris regime long crack. Validation of the fracture mechanics-based approach for various materials and notch geometries is limited.

The objective of this paper is to develop a general methodology for fatigue analysis of notched specimens and validate this methodology for various materials and notch geometries. The current focus is on the fatigue limit prediction of notched specimen with various notch geometries. An asymptotic interpolation method is proposed to estimate the stress intensity factor (SIF) solution for cracks at the notch root. Both edge notched and center notched specimens with finite dimension correction are included into the proposed method. The small crack correction is introduced inspired by the Kitagawa–Takahashi diagram [27] and the El Haddad's small crack correction [28] for smooth specimen. It is assumed that all specimens in the current investigation contain an edge-through notch crack. The fatigue limit of notched specimens is estimated using the proposed SIF solution when the crack length is approaching zero. A wide range of material data available in the literature are used to validate the proposed methodology.

2. Fatigue limit prediction methodology

2.1. Asymptotic solution for stress intensity factor considering notch effect

The stress intensity factor solution is required for fatigue crack growth and life prediction using the fracture mechanics-based approach. Two examples of SIF solution of a crack at notch root have been shown in Section 1. Eq. (7) is proposed by Kujawski [14] and includes the stress concentration factor K_t of the notch. The drawback is that it predicts a zero SIF value when the crack length is long (i.e., $\frac{a}{\rho} \rightarrow \infty$). Under these conditions, the notch effect disappears but the SIF solution should not be zero since the crack length is not zero. Eq. (8) was proposed for cracks at the notch root in a center notched component [15] and not for the other notch geometries, such as edge notched specimen. In view of this, a new calculation procedure is proposed here. Jergéus [29] and Härkegård [30] proposed an asymptotic interpolation method for SIF solution of the crack at the notch root of an edge notched specimen. A similar approach was proposed by Wormsen et al. [31]. All these approaches assume edge-through cracks in a semi-infinite plate. The general idea is to match two extreme cases. One is for the short crack solution and the other is for the long crack solution. The SIF formula asymptotically matches these two extremes and the SIF solutions between these two extremes are interpolated. This approach is first illustrated assuming a through crack on the surface of an edge notch in a semi-infinite plate. Detailed derivation and verification of the asymptotic interpolation can be found in [31]. The general formula for the SIF solution is expressed as

$$K = 1.122\sigma \sqrt{\pi \left(a + d \left\{ 1 - \exp \left[-\frac{a}{d} (K_t^2 - 1) \right] \right\} \right)} \quad (10)$$

where a is the crack length, d is the notch depth, K_t is the stress concentration factor, and 1.122 is the surface correction factor. The SIF solution (Eq. (10)) under several extreme conditions is discussed here.

For a short crack ($\frac{a}{d} \rightarrow 0$), $\frac{a}{d}(K_t^2 - 1)$ is approaching zero for a finite stress concentration factor. Using the first order Taylor series expansion of the exponential function

$$\exp\left[-\frac{a}{d}(K_t^2 - 1)\right] = 1 - \frac{a}{d}(K_t^2 - 1) \quad (11)$$

Eq. (10) can be expressed as

$$K = 1.122K_t\sigma\sqrt{\pi a} \quad (12)$$

For a long crack ($\frac{a}{d} \rightarrow \infty$), $\frac{a}{d}(K_t^2 - 1)$ is approaching infinity when the stress concentration factor does not equal to unity. When the exponential function $\exp[-\frac{a}{d}(K_t^2 - 1)]$ approaches zero, Eq. (10) can be expressed as

$$K = 1.122\sigma\sqrt{\pi(a+d)} \quad (13)$$

Comparing Eqs. (12) and (13), it is seen that the asymptotic solution matches the two extreme cases for a short crack and a long crack at notch root. Eq. (12) is for the case of a short crack. In this case, the existence of notch increases the local stress field of the crack tip and the stress intensity factor solution is governed by the notch stress ($K_t\sigma$). Eq. (13) is for the case of a long crack. In this case, the crack tip is beyond the notch-affected region and the existence of notch increase the effective length of the crack. A schematic plot for these two extreme cases is shown in Fig. 1.

Next, the discussion is extended to the notched specimen with finite dimensions. A finite dimension correction factor is introduced to modify Eq. (10) as

$$K = 1.122\alpha\sigma\sqrt{\pi\left(a+d\left\{1 - \exp\left[-\frac{a}{d}\left(\frac{K_t^2}{\alpha^2} - 1\right)\right]\right\}\right)} \quad (14)$$

where α is the correction factor for an edge crack with length of $(a+d)$ in a finite dimension specimen. Formulas for α can be found in handbooks [32] of the stress analysis of cracks for commonly used specimen types, such as those listed later in this paper. If the function is not readily available in the literature or textbook, numerical methods, such as finite element method, can be used to obtain this function.

For a short crack ($\frac{a}{d} \rightarrow 0$), the SIF solution is same as Eq. (12) since the finite dimension correction is unity for a very small crack. For a long crack ($\frac{a}{d} \rightarrow \infty$), Eq. (14) can be expressed as

$$K = 1.122\alpha\sigma\sqrt{\pi(a+d)} \quad (15)$$

Eq. (14) is the proposed SIF solution for a crack at the notch root of a general edge notched specimen.

Similar asymptotic interpolation for center notched specimen can be also developed. Let us first consider an infinite plate with a center notch. Two different crack configurations for a center notched specimen are considered, i.e. a single edge-through crack and a pair of edge-through cracks. A schematic representation of two different crack configurations is shown in Fig. 2. The derivation for these two different crack configurations has very similar procedures with a slight different solution.

Case 1: Single edge-through crack

For a small crack ($\frac{a}{d} \rightarrow 0$) at the notch root of a center notched specimen, the SIF solution is the same as that of Eq. (12) since the crack is under the notch stress region and the surface correction factor 1.122 still applies to the SIF solution. For a

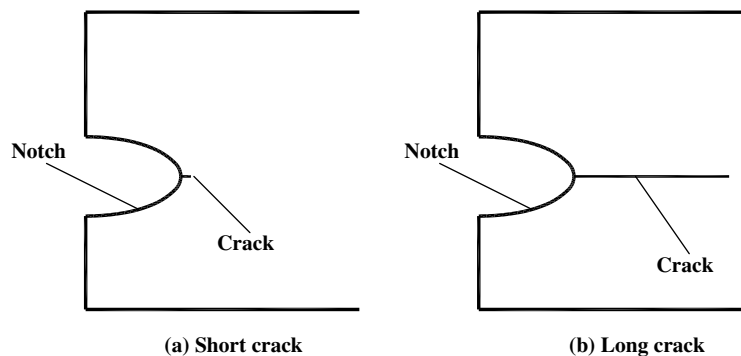


Fig. 1. Schematic plot of shallow notch and deep notch with a crack at the notch root.

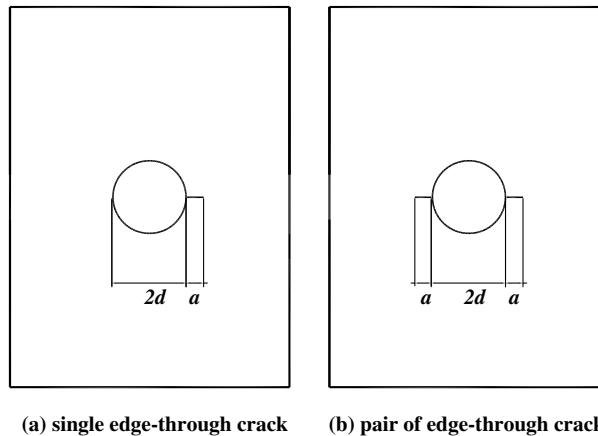


Fig. 2. Schematic plot of different crack configuration.

long crack ($\frac{a}{d} \rightarrow \infty$), the SIF solution becomes that of a center crack with half length of $(a + 2d)/2$ in an infinite plate. The SIF solution can be expressed as

$$K = \frac{\sigma}{\sqrt{2}} \sqrt{\pi(a + 2d)} \quad (16)$$

To satisfy these two extreme cases, a modification of Eq. (10) is proposed as

$$K = 1.122\beta\sigma\sqrt{\pi\left(a + 2d\left\{1 - \exp\left[-\frac{a}{2d}(K_t^2 - 1)\right]\right\}\right)} \quad (17)$$

where β is

$$\beta = \frac{1}{1.122\sqrt{2} - (1.122\sqrt{2} - 1)\exp(-\sqrt{\frac{a}{d}})} \quad (18)$$

The proposed formula (Eq. (17)) is compared with the solution of a single edge-through crack from a center circular hole reported in [33]. The SIF solution in [33] can be expressed as

$$K = 1.122f\sigma\sqrt{\pi a} \quad (19)$$

$$f = \left(1 + \frac{0.2}{1 + \frac{a}{d}} + \frac{0.3}{(1 + \frac{a}{d})^6}\right) \left(2 - 2.354\frac{\frac{a}{d}}{1 + \frac{a}{d}} + 1.2056\left(\frac{\frac{a}{d}}{1 + \frac{a}{d}}\right)^2 - 0.2211\left(\frac{\frac{a}{d}}{1 + \frac{a}{d}}\right)^3\right) \quad (20)$$

The proposed formula (Eq. (17)) gives the SIF estimation within 4% error, compared to the reference solution [33]. Comparing Eqs. (10) and (17), the edge notched specimen and center notched specimen differ with each other when the crack length is large compared to the notch size. However, they both give the same solution when the crack is very small compared to the notch size (Eq. (12)).

Similar method to include the finite dimension correction factor can be used for center notched specimen following the same procedure for edge notched specimen. Eq. (17) can be rewritten as

$$K = 1.122\alpha\beta\sigma\sqrt{\pi\left(a + 2d\left\{1 - \exp\left[-\frac{a}{2d}\left(\frac{K_t^2}{\alpha^2} - 1\right)\right]\right\}\right)} \quad (21)$$

where α is the correction factor for a center crack with length of $(a + 2d)$ in a finite dimension specimen. Eq. (21) is the proposed formula for SIF estimation for a single edge-through crack of center notched specimens. Eq. (21) is used in the experimental model validation section.

Case 2: A pair of edge-through cracks

The derivation of a pair of edge-through cracks in a center notched specimen is very similar to that of a single edge-through crack. Only the main formulas are listed here.

For a sufficiently shallow crack, the K value is the same as that of Eq. (12). A K solution that asymptotically satisfy the short and long crack solution can then be expressed as

$$K = 1.122\beta\sigma\sqrt{\pi\left(a + d\left\{1 - \exp\left[-\frac{a}{d}(K_t^2 - 1)\right]\right\}\right)} \quad (22)$$

where β is

$$\beta = \frac{1}{1.122 - (1.122 - 1) \exp(-\sqrt{\frac{a}{d}})} \quad (23)$$

Comparing Eqs. (17), (18) to Eqs. (22), (23), it is shown that the main difference between two sets of formulas is the multiplication factor (e.g., 2 and 1 in Eqs. (17) and (22)). The multiplication factor is 2 for the single edge-through crack and is 1 for a pair of edge-through cracks.

Eq. (22) is compared with the following expression for a semi-infinite center notched specimen [34]

$$K = 0.5 \left(3 - \frac{a}{a+d} \right) \left[1 + 1.243 \left(1 - \frac{a}{a+d} \right)^3 \right] \sigma \sqrt{\pi a} \quad (24)$$

The maximum difference was found to be 3.1%.

The proposed solution is originally developed for holes and U notched specimen. For V notched specimen, different formulas may be required. However, as shown in [31,35], the V notch behaves like a U notch when the open angle is less than 90°. In the experimental validation of this paper, both U notched and V notched bar are used and the proposed formula works well. For the V notched specimen with large open angles, future study is required.

2.2. Stress intensity factor with small crack correction

An important concept in classical fatigue theory ($S-N$ type) is the fatigue limit, which defines a loading criterion under which no macroscopic crack will form or the initiated crack will be arrested. Similarly, the concept of fatigue crack threshold is important for fracture mechanics-based fatigue analysis, which defines a loading criterion under which the cracks will not grow significantly. A link between the traditional safe-life design approach and damage tolerance design approach has been proposed and is known as the Kitagawa–Takahashi (KT) diagram [27]. A schematic plot of the KT diagram is shown in Fig. 3. According to the KT diagram, the fatigue limit of specimen increases as the crack size decreases. The fatigue limit remains constant when the crack size is below a certain value, which is determined by fatigue limit and the fatigue crack threshold intensity factor using linear elastic fracture mechanics (LEFM). El Haddad et al. [28] proposed a model to express the fatigue limit $\Delta\sigma_f$ using the fatigue threshold stress intensity factor ΔK_{th} and a fictional crack length a .

$$\Delta K_{th} = \Delta\sigma_f \sqrt{\pi a_0} \quad (25)$$

Eq. (25) refers to an infinite plate with a centered through crack of length $2a_0$. The well-known El Haddad model for the stress intensity factor considering the small crack effect was proposed as

$$\Delta K = \Delta\sigma_f \sqrt{\pi(a + a_0)} \quad (26)$$

where a_0 is the characteristic crack length of the material and can be expressed as

$$a_0 = \frac{1}{\pi} \left(\frac{\Delta K_{th}}{\Delta\sigma_f} \right)^2 \quad (27)$$

The fatigue limit condition is obtained when the modified stress intensity factor equals to the material threshold stress intensity factor, i.e.

$$\Delta K = \Delta\sigma_f \sqrt{\pi(a + a_0)} = \Delta K_{th} = \Delta\sigma_f \sqrt{\pi a_0} \quad (28)$$

The original El Haddad's model is for a center crack in an infinite plate. It has been extended to consider an edge crack with the surface correction of 1.122 [7,36]. Eqs. (26), (27) are modified as

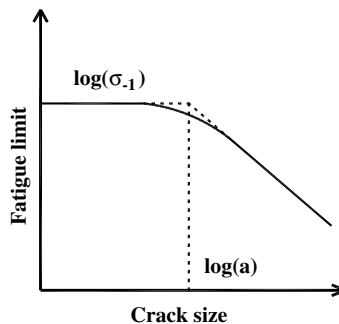


Fig. 3. Schematic representation of the Kitagawa–Takahashi diagram.

$$\Delta K = 1.122\Delta\sigma_f\sqrt{\pi(a+a_0)} \quad (29)$$

where a_0 is the characteristic crack length of the material and can be expressed as

$$a_0 = \frac{1}{\pi} \left(\frac{\Delta K_{th}}{1.122\Delta\sigma_f} \right)^2 \quad (30)$$

The key idea in the El Haddad's small crack correction is to replace the original real crack length (a) by an effective crack length ($a+a_0$) in the SIF solution. When the real crack length is approaching zero, the fatigue limit of the specimen is approaching that of a smooth specimen without crack.

A SIF solution was proposed for cracks at the notch root for both edge notched specimen and center notched specimen in Section 2.1. The similar idea of El Haddad's model can be extended to notched specimen also. The effect of small crack is included by replacing the crack length (a) by an effective crack length ($a+a_0$) in the notch crack SIF solution. For edge notched specimen, Eq. (14) can be modify as

$$\Delta K = 1.122\alpha\Delta\sigma\sqrt{\pi\left(a+a_0+d\left\{1-\exp\left[-\frac{a+a_0}{d}\left(\frac{K_t^2}{\alpha^2}-1\right)\right]\right\}\right)} \quad (31)$$

In Eq. (31), the stress intensity factor K and stress σ are changed to stress intensity factor range ΔK and stress range $\Delta\sigma$ for the fatigue analysis.

Similar extension can be applied to center notched specimen. Eq. (21) is modified as

$$\Delta K = 1.122\alpha\beta\Delta\sigma\sqrt{\pi\left(a+a_0+2d\left\{1-\exp\left[-\frac{a+a_0}{2d}\left(\frac{K_t^2}{\alpha^2}-1\right)\right]\right\}\right)} \quad (32)$$

where β is

$$\beta = \frac{1}{1.122\sqrt{2} - (1.122\sqrt{2} - 1)\exp\left(-\sqrt{\frac{a+a_0}{d}}\right)} \quad (33)$$

Eqs. (31) and (32) are the proposed stress intensity factor range considering the small crack correction for notched specimens. The characteristic crack length in the proposed method includes the surface correction factor of 1.122 and Eq. (30) is used.

2.3. Fatigue limit prediction of notched specimens

Combining the methods described in Sections 2.1 and 2.2, fatigue limit of notched specimen can be calculated following the same procedure of El Haddad's model. When the realistic crack length approaches zero, the SIF factor solution with small crack correction (Eqs. (31), (32)) approaches the fatigue limit of the notched specimen. The limit state function for an edge notched specimen can be written as

$$\Delta K = 1.122\alpha\Delta\sigma\sqrt{\pi\left(a_0+d\left\{1-\exp\left[-\frac{a_0}{d}\left(\frac{K_t^2}{\alpha^2}-1\right)\right]\right\}\right)} = \Delta K_{th} = 1.122\Delta\sigma_f\sqrt{\pi a_0} \quad (34)$$

In Eq. (34), all terms of the real crack length a disappear because the crack length a is approaching zero. Eq. (34) can be rewritten as

$$\frac{\Delta\sigma}{\Delta\sigma_f} = \frac{1}{\alpha} \frac{1}{\sqrt{\left(1+\frac{d}{a_0}\left\{1-\exp\left[-\frac{a_0}{d}\left(\frac{K_t^2}{\alpha^2}-1\right)\right]\right\}\right)}} \quad (35)$$

where α is the finite dimension correction factor for an edge crack with length of (a_0+d) in a finite dimension specimen.

Similar results can be obtained for single edge-through crack of a center notched specimen as

$$\frac{\Delta\sigma}{\Delta\sigma_f} = \frac{1}{\alpha} \frac{1}{\beta} \frac{1}{\sqrt{\left(1+\frac{2d}{a_0}\left\{1-\exp\left[-\frac{a_0}{2d}\left(\frac{K_t^2}{\alpha^2}-1\right)\right]\right\}\right)}} \quad (36)$$

where β is

$$\beta = \frac{1}{1.122\sqrt{2} - (1.122\sqrt{2} - 1)\exp\left(-\sqrt{\frac{a_0}{d}}\right)} \quad (37)$$

Eqs. (35) and (36) are the proposed formula for fatigue limit prediction of notched specimen. As can be seen from these two equations, the fatigue limit of notched specimen depends on both material properties and notch geometries.

3. Discussion of the proposed methodology

The relationship between the proposed methodology and the traditionally used fatigue notch factor approach is discussed below.

From Eqs. (2)–(4), it is seen that the fatigue notch factor is related to the notch sensitivity factor, which is merely an empirical quantity describing the experimentally determined fatigue limit strength. Unfortunately, the relationship of notch size with fatigue notch factor K_f does not follow the same trend for all materials. Extensive test data for different combinations of notch depth and notch root radius are required to obtain notch sensitivity factor for a given material, which is expensive and time consuming. Also, empirical fitting procedure to calculate the fatigue notch factor K_f introduces additional uncertainties in reliability estimation [37]. For the above mentioned reason, Ren and Nicholas [37] stated that the fatigue notch factor is not completely predictable.

In the proposed method (Eqs. (35), (36)), the fatigue notch factor correlates with both specimen geometries (notch depth, notch radius and specimen width) and material properties (fatigue limit and fatigue crack threshold stress intensity factor).

Eq. (1) shows the original definition of the fatigue notch factor. The proposed fatigue limits prediction formula (Eqs. (35) and (36)) can be used to predict the fatigue notch factor. Fatigue notch factor of an edge notched specimen can be written as

$$K_f = \frac{\Delta\sigma_f}{\Delta\sigma} = \alpha \sqrt{\left(1 + \frac{d}{a_0} \left\{1 - \exp\left[-\frac{a_0}{d} \left(\frac{K_t^2}{\alpha^2} - 1\right)\right]\right\}\right)} \quad (38)$$

Fatigue notch factor of a center notched specimen can be written as

$$K_f = \frac{\Delta\sigma_f}{\Delta\sigma} = \alpha\beta \sqrt{\left(1 + \frac{2d}{a_0} \left\{1 - \exp\left[-\frac{a_0}{2d} \left(\frac{K_t^2}{\alpha^2} - 1\right)\right]\right\}\right)} \quad (39)$$

Eqs. (38) and (39) can be used to predict the fatigue notch factor of the specimen. Several extreme cases for edge notched specimen are discussed here. If the characteristic crack length is very small compared to the notch depth ($\frac{a_0}{d} \rightarrow 0$) and the stress concentration factor is a finite number ($K_t^2 - 1 \neq \infty$), Eq. (38) becomes

$$K_f = \frac{\Delta\sigma_f}{\Delta\sigma} = K_t \quad (40)$$

This case corresponds to the full notch sensitivity, i.e. the fatigue notch factor is the same as the theoretical stress concentration factor. Another extreme case is when the crack length is very large compared to the notch depth ($\frac{a_0}{d} \rightarrow \infty$) and the stress concentration factor is not unity ($K_t \neq 1$). Eq. (38) becomes

$$K_f = \frac{\Delta\sigma_f}{\Delta\sigma} = \alpha \sqrt{1 + \frac{d}{a_0}} \approx \sqrt{1 + \frac{d}{a_0}} \approx 1 \quad (41)$$

In Eq. (41), the finite dimension correction factor is approximately unity because the characteristic crack length is usually very small (in the magnitude of microns) compared to the specimen dimension (in the magnitude of millimeters or larger). In this case, the fatigue notch factor is close to unity. A typical example is listed in the collected experimental data (see Table 1; the third row for Annealed 0.45 carbon steel). The notch depth for this specimen is 0.005 mm and is relatively small compared to the characteristic crack length (about 0.05 mm). The stress concentration factor is 2.54 and the predicted fatigue notch factor is 1.04. The experimental obtained fatigue notch factor for this specimen is 1.06. The model prediction of the fatigue notch factor under different stress concentration factors are shown in Fig. 4 as a function of $\frac{a_0}{d}$. The x -axis is $\frac{a_0}{d}$ in log scale and the y -axis is the fatigue notch factor. It is clearly seen that the proposed model gives two asymptotic values of the fatigue notch factor, i.e. one is approaching K_t and the other is approaching unity.

Above discussion focuses on the effect of the ratio of $\frac{a_0}{d}$. Another factor in the proposed model is the elastic stress concentration factor K_t . Its effects on the fatigue notch factor are discussed below. One extreme case is that the K_t is approaching unity. Eq. (38) becomes

$$K_f = \frac{\Delta\sigma_f}{\Delta\sigma} = K_t \approx 1 \quad (42)$$

Eq. (42) shows that the fatigue notch factor is approaching unity when the stress concentration factor is approaching unity, which is not surprising since the specimen becomes a smooth specimen and the ratio of fatigue limits should be unity. Another extreme case is that the K_t is approaching infinity, which is for very sharp notches. Eq. (38) becomes

$$K_f = \frac{\Delta\sigma_f}{\Delta\sigma} = \alpha \sqrt{1 + \frac{d}{a_0}} \quad (43)$$

Table 1

Detailed experimental data of notched specimens

Material (specimen) stress ratio	d (mm)	ρ (mm)	W (mm)	$\Delta\sigma$ (MPa)	K_t^*	Exp. K_f	Pre. K_f^{**}
Annealed 0.45 carbon steel (CNBB) $R = -1$	0.005	0.050	5.010	547.000	1.680	1.064	1.0644
	0.005	0.020	5.010	547.000	2.070	1.064	1.0644
	0.005	0.020	5.010	557.000	2.540	1.0449	1.0644
	0.010	0.050	5.020	484.000	1.970	1.2025	1.114
	0.010	0.020	5.020	494.000	2.550	1.1781	1.114
	0.010	0.010	5.020	484.000	3.230	1.2025	1.114
	0.100	0.600	5.200	373.000	1.780	1.5603	1.5587
	0.100	0.300	5.200	338.000	2.130	1.7219	1.6807
	0.100	0.100	5.200	302.000	3.060	1.9272	1.7979
	0.100	0.050	5.200	320.000	3.980	1.8188	1.8114
	0.100	0.020	5.200	320.000	5.860	1.8188	1.8122
	0.500	0.600	6.000	208.000	3.210	2.7981	2.8382
	0.500	0.300	6.000	174.000	4.130	3.3448	3.3125
	0.500	0.310	6.000	162.000	6.570	3.5926	3.8817
	0.500	0.050	6.000	162.000	8.970	3.5926	3.9764
	0.500	0.020	6.000	168.000	13.700	3.4643	3.9841
	0.500	0.010	6.000	168.000	19.000	3.4643	3.9841
	1.500	0.600	8.000	85.400	7.820	6.815	6.8914
	1.500	0.300	8.000	68.400	10.300	8.5088	8.2548
	1.500	0.100	8.000	61.000	16.700	9.541	9.9317
1.500	0.050	8.000	61.000	23.200	9.541	10.246	
1.500	0.020	8.000	61.000	36.000	9.541	10.273	
1.500	0.010	8.000	63.500	50.400	9.1654	10.273	
Annealed 0.36 carbon steel*** (CNBB) $R = -1$	0.100	0.200	13.200	168.000	2.400	1.5929	1.547
	0.150	0.200	13.300	168.000	2.740	1.7698	1.7531
	0.300	0.200	13.600	162.000	3.580	2.1238	2.2731
	0.500	0.200	14.000	162.000	4.470	2.7531	2.851
	0.700	0.200	14.400	174.000	5.290	3.1631	3.3748
	1.000	0.200	15.000	208.000	6.450	4.018	4.1169
SAE 1045 steel (CNPT) $R = 0$	0.120	0.120	44.450	325.000	3.000	1.3785	1.6295
	0.250	0.250	44.450	308.000	3.000	1.4545	2.0216
	0.500	0.500	44.450	270.000	3.010	1.6593	2.322
	1.500	1.500	44.450	212.000	3.020	2.1132	2.6365
	2.500	2.500	44.450	209.000	3.040	2.1435	2.7457
SAE 1045 steel (CNPT) $R = -1$	0.120	0.120	44.450	357.000	3.000	1.6975	1.6704
	0.250	0.250	44.450	306.000	3.000	1.9804	2.0565
	0.500	0.500	44.450	273.000	3.010	2.2198	2.3481
	1.500	1.500	44.450	231.000	3.020	2.6234	2.6511
	2.500	2.500	44.450	232.000	3.040	2.6121	2.7568
2024-T351 Al alloy (CNPT) $R = 0$	0.120	0.120	44.450	172.000	3.000	1	1.1961
	0.250	0.250	44.450	113.000	3.000	1.5221	1.579
	0.500	0.500	44.450	107.000	3.010	1.6075	1.9601
	1.500	1.500	44.450	85.800	3.020	2.0047	2.4235
2024-T351 Al alloy (CNPT) $R = -1$	0.120	0.120	44.450	159.000	3.000	1.5597	1.4715
	0.250	0.250	44.450	123.000	3.000	2.0163	1.8777
	0.500	0.500	44.450	121.000	3.000	2.0496	2.2066
	1.500	1.500	44.450	83.800	3.000	2.9594	2.5586
G40.11 steel (CNPT) $R = -1$	0.200	0.200	70.000	336.000	3.000	1.6071	1.5524
	0.480	0.480	70.000	239.000	3.000	2.2594	2.0237
	4.800	4.800	70.000	205.000	3.000	2.6341	2.7126
SM41B steel (CNPT) $R = -1$	3.000	0.160	45.000	95.300	9.780	3.4208	3.6148
	3.000	0.390	45.000	104.000	6.600	3.1346	3.4791
	3.000	0.830	45.000	95.300	4.880	3.4208	3.1439
	3.000	3.000	45.000	128.000	3.000	2.5469	2.3201
SM41B steel (CNPT) $R = 0$	3.000	0.160	45.000	63.300	9.780	4.3286	4.5033
Mild steel (0.15% C) (CNBT) $R = -1$	5.080	0.050	43.000	68.800	24.000	6.1047	5.4368
	5.080	0.100	43.000	70.000	17.100	6	5.4367
	5.080	0.130	43.000	67.700	15.400	6.2038	5.4361
	5.080	0.250	43.000	68.800	11.300	6.1047	5.407
	5.080	0.640	43.000	68.800	7.540	6.1047	5.0599
	5.080	1.270	43.000	77.000	5.660	5.4545	4.4763
	5.080	5.080	43.000	121.000	3.260	3.4711	3.0407

(continued on next page)

Table 1 (continued)

Material (specimen) stress ratio	d (mm)	ρ (mm)	W (mm)	$\Delta\sigma$ (MPa)	K_t^*	Exp. K_f	Pre. K_f^{**}
Mild steel (0.15% C) (DNPT) $R = -1$	5.080	0.100	64.000	84.100	14.900	4.9941	4.7868
	5.080	0.250	64.000	90.900	9.750	4.6205	4.7555
	5.080	0.500	64.000	84.100	7.250	4.9941	4.5643
	5.080	1.270	64.000	104.000	4.750	4.0385	3.8375
	5.080	7.620	64.000	156.000	2.500	2.6923	2.3813
NiCr steel (CNBT) $R = -1$	0.510	0.130	22.600	236.000	5.050	4.2373	3.444
	5.080	0.050	43.000	88.600	24.000	11.287	12.435
	5.080	0.130	31.800	96.600	17.300	10.352	12.319
2.25Cr-1 mo steel (CNBT) $R = -1$	0.030	0.030	5.000	429.000	3.060	1.0256	1.1059
	0.050	0.050	5.000	403.000	3.070	1.0918	1.1592
	0.070	0.070	5.000	321.000	3.090	1.3707	1.2111
	0.200	0.200	5.000	237.000	3.170	1.8565	1.5262
	0.400	0.400	5.000	209.000	3.320	2.1053	1.9792
	0.760	0.760	5.000	155.000	3.860	2.8387	2.8169
304 stainless steel (CNBT) $R = -1$	5.080	0.050	43.000	72.300	24.000	9.9585	9.705

* All the stress concentration factor values are referred to the gross cross section.

** The predicted fatigue notch factor are obtained using Eq. (38) for CNBB, CNBT, and DNPT specimen or Eq. (39) for CNPT specimen.

*** The experimental data reported in the table format by Atzori et al. [36] is not consistent with the data reported in the graphic format. The data in the graphic format is used.

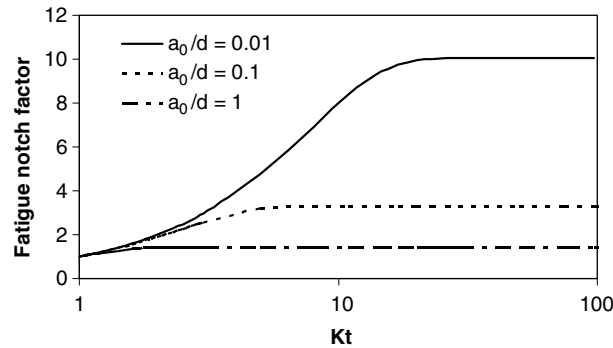


Fig. 4. Fatigue notch factor variation corresponding to stress concentration factor under several $\frac{a_0}{d}$ ratios.

Eq. (43) indicates that the fatigue notch factor will not approach infinity as the stress concentration factor is approaching infinity. Instead, it is approaching a constant value, which is determined by the ratio of notch depth to the characteristic crack length. A typical example is shown in the collected experimental data (see Table 2; the last row for Annealed 0.45 carbon steel). The stress concentration factor is 50.4 and can be considered very large. The model predicts the fatigue notch factor is 10.27 and the experimental fatigue notch factor is 9.17. This agrees with the results in [28,38] that the fatigue limit approaches a constant by keeping the notch depth constant and increasing the stress concentration factor K_t . The fatigue notch factor variation corresponding to different stress concentration factors are shown in Fig. 5 for several fixed $\frac{a_0}{d}$ ratios. The x-axis is the stress concentration factor in log scale and the y-axis is the fatigue notch factor. In Fig. 5, the finite dimension correction factor is assumed to be unity for a semi-infinite plate. As shown in Fig. 5, the proposed method predicts the fatigue notch factor has two asymptotic values corresponding to different stress concentration factors, i.e. one extreme case is unity and the other is $\sqrt{1 + \frac{d}{a_0}}$.

The above discussions are for extreme cases and the cases between those extremes are interpolated using the proposed formula. In Section 4, it is shown that proposed methodology works well for various types of notch geometries and materials.

4. Experimental validation of fatigue limit prediction

A wide range of material data available in the literature is collected and used to validate the proposed methodology. The collected data include various types of aluminums and steels. The experimental data is reported by Atzori et al. [36]. A detailed description of material properties is listed in Table 2. The notched specimens and fatigue loading types of collected materials can be grouped into four categories: circumferential V-shaped notch in a round bar under remote bending (CNBB); circumferential V-shaped notch in a round bar under remote tension (CNBT); center notched plate under remote tension (CNPT); double edge notched plate under remote tension (DNPT). A schematic plot of these four types of specimen and

Table 2
Material properties

Material name	Yield strength σ_y (MPa)	Fatigue limit $\Delta\sigma_f$ (MPa)	Fatigue threshold stress intensity factor ΔK_{th} (MPa m ^{0.5})	Stress ratio R
Annealed 0.45 carbon steel	364	582	8.1	-1
Annealed 0.36 carbon steel	N/A	446	7.6	-1
SAE 1045 steel	466	448	6.9	0
SAE 1045 steel	466	606	9	-1
2024-T351 Al alloy	360	172	4	0
2024-T351 Al alloy	360	248	4.4	-1
G40.11 steel	376	540	11.5	-1
SM41B steel	194	326	12.36	-1
	194	274	8.36	0
Mild steel (0.15% C)	340	420	12.8	-1
NiCr steel	834	1000	12.8	-1
2.25Cr-1 mo steel	380	440	12	-1
304 stainless steel	222	720	12	-1

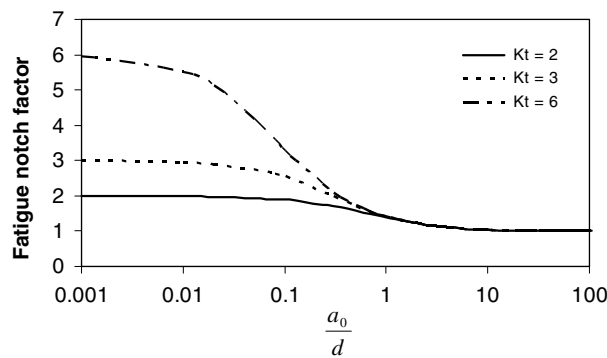


Fig. 5. Fatigue notch factor variation corresponding to $\frac{a_0}{d}$ ratios under several stress concentration factors.

loading is shown in Fig. 6. A detailed list of the experimental observation and geometry properties of specimens is listed in Table 1. In Table 1, “Exp” refers to the experimental observations and “Pre” refers to model predictions.

In the proposed methodology, the stress concentration factor K_t and finite dimension correction factor α are required. The stress concentration factor can be obtained from available handbooks [39]. It should be noted that the stress concentration

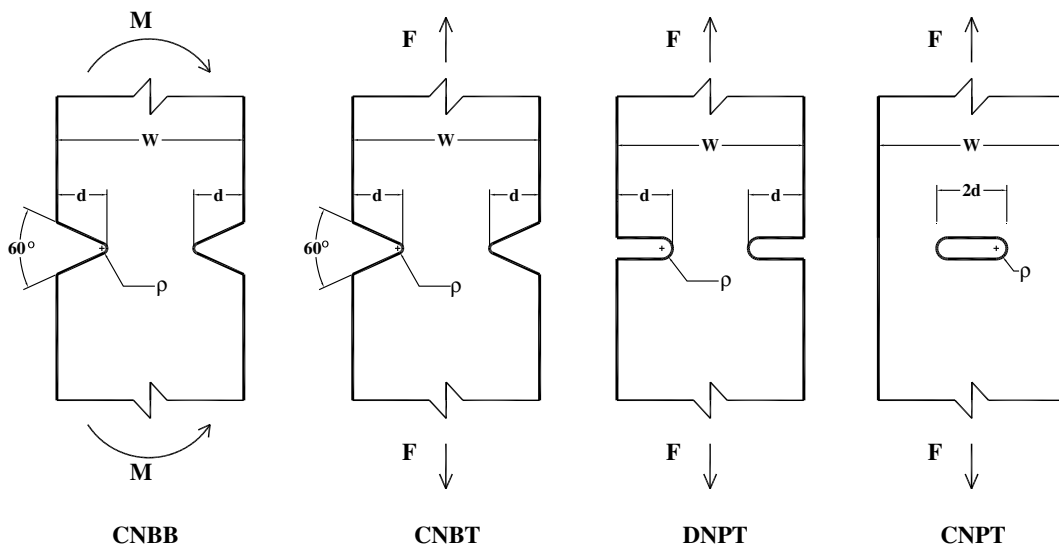


Fig. 6. Geometry of notched specimen.

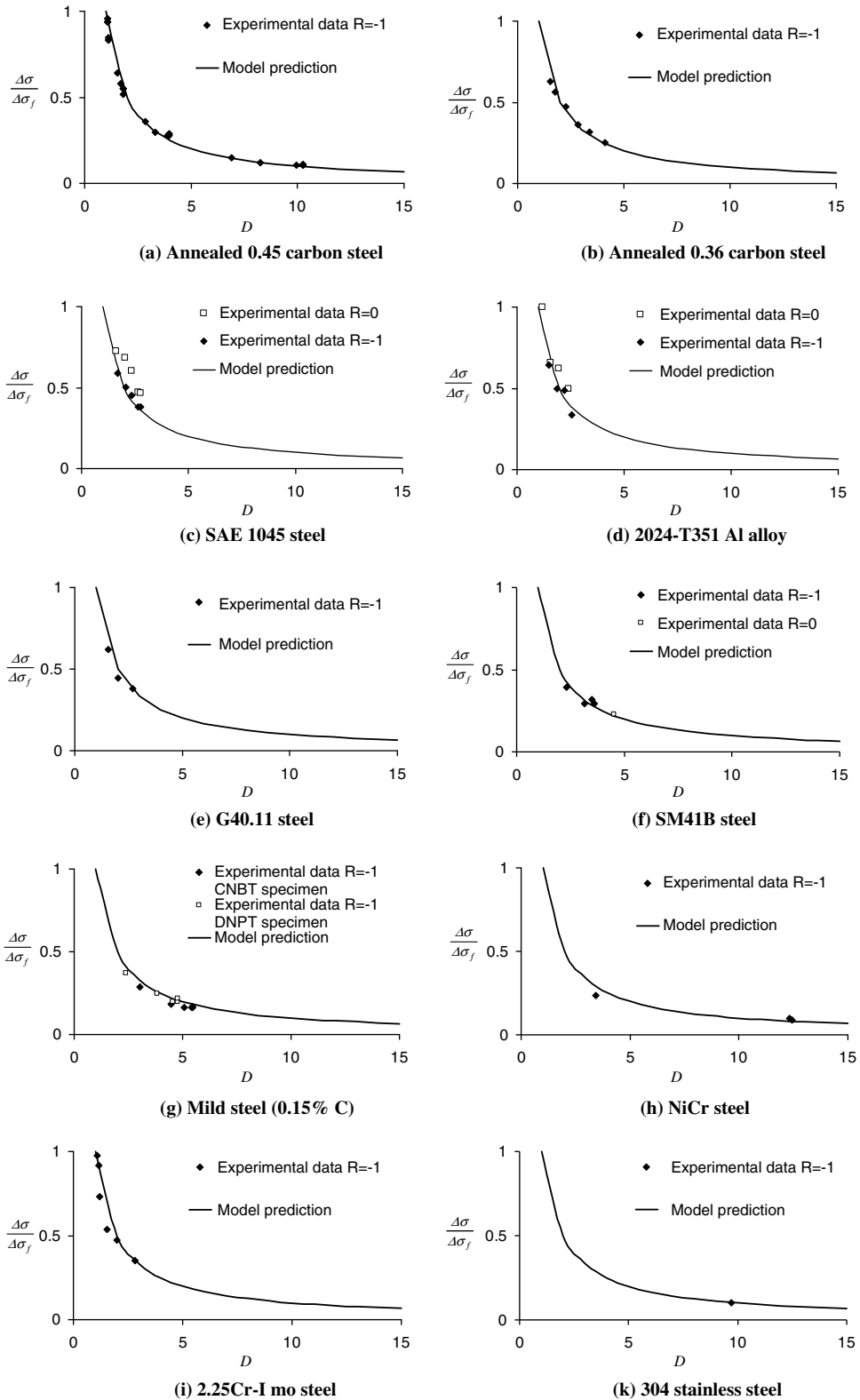


Fig. 7. Comparison of experimental data and model prediction for individual materials.

factor used in this method is the one referred to the remote gross cross section stress rather than the net cross section stress. The K_t factor is reported by Atzori et al. [36] and the values listed in Table 2 are used. The finite dimension correction factor α in the proposed method can be obtained from fracture mechanics textbooks or obtained from finite element analysis if analytical or empirical solution is not available. In this paper, the empirical solutions available in the literature are used. For CNBB, the solution from [40] is expressed as:

$$\alpha = \frac{1}{1.122} \frac{3}{8} \xi^{-5/2} \left(1 + \frac{1}{2} \xi + \frac{3}{8} \xi^2 + \frac{5}{16} \xi^3 + \frac{35}{128} \xi^4 + 0.531 \xi^5 \right), \quad \xi = 1 - 2 * (d + a_0) / W \quad (44)$$

For CNBT, the solution from [41] is expressed as:

$$\alpha = \frac{1}{1.122} \frac{1}{2} \xi^{-1/2} \left(\xi + \frac{1}{2} \xi + \frac{3}{8} \frac{1}{\xi} - \frac{5}{14} \frac{1}{\xi^2} + \frac{11}{15} \frac{1}{\xi^3} \right), \quad \xi = W / (W - 2 * (d + a_0)) \quad (45)$$

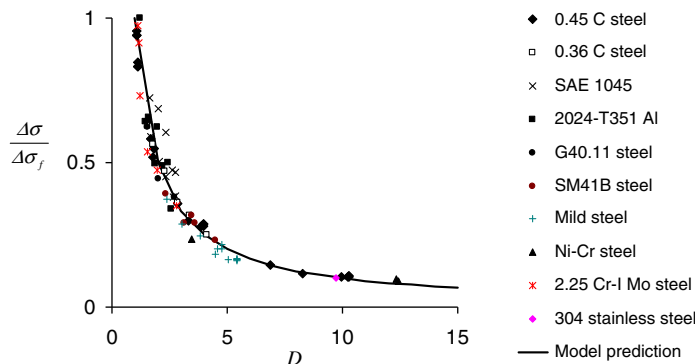
For CNPT, the solution from [41] is expressed as:

$$\alpha = \sec \left(\frac{\pi}{2} \xi \right), \quad \xi = 2 * (d + a_0) / W \quad (46)$$

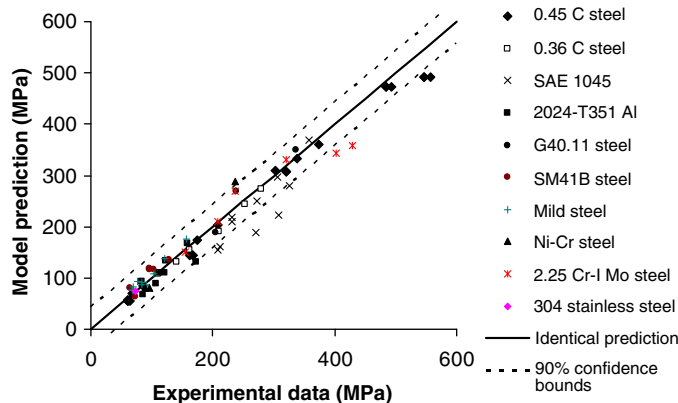
For DNPT, the solution from [41] is expressed as:

$$\alpha = \frac{1}{1.12} (1.12 + 0.41 \xi - 4.78 \xi^2 + 15.44 \xi^3), \quad \xi = 2 * (d + a_0) / W \quad (47)$$

Once all required material property and mechanical parameters are obtained, the fatigue limit of notched specimen can be calculated using Eq. (35) for edge notched specimen and Eq. (36) for center notched specimen. The model prediction and experimental data are shown in Fig. 7 for each material. In Fig. 7, the x-axis is the non-dimensional parameter D , where D is $\alpha \sqrt{\left(1 + \frac{d}{a_0} \left\{ 1 - \exp \left[-\frac{a_0}{d} \left(\frac{K_t^2}{\alpha^2} - 1 \right) \right] \right\} \right)}$ for edge notched specimen or $\alpha \beta \sqrt{\left(1 + \frac{2d}{a_0} \left\{ 1 - \exp \left[-\frac{a_0}{2d} \left(\frac{K_t^2}{\alpha^2} - 1 \right) \right] \right\} \right)}$ for center



(a) fatigue notch factor comparison



(b) fatigue limit prediction comparison

Fig. 8. Comparison between experimental data and model prediction for all materials.

notched specimen and the y -axis is the normalized fatigue limit $\frac{\Delta\sigma}{\Delta\sigma_f}$. An overall comparison for all materials is shown in Fig. 8a. From Figs. 7 and 8a, it is seen that the proposed model agrees with experimental results very well.

Comparisons between predicted fatigue limits and experimental observations for all materials are plotted in Fig. 8b. The x -axis is experimental observation and the y -axis is the model prediction. The solid line indicates that prediction results and experimental data are identical. The 90% confidence bounds are also plotted as dashed lines in Fig. 8b. The confidence bounds are calculated as follows. The differences between experimental observation and model prediction are fitted to a Gaussian distribution. Once the probability distribution is obtained, the confidence bounds can be easily calculated using statistics. A very good agreement is observed. A few model predictions are outside the confidence bounds but are on the conservative side.

5. Conclusion

A general methodology for fatigue analysis of notched specimens is proposed in this paper. The methodology is based on an asymptotic SIF solution for cracks at the notch root and the Kitagawa–Takahashi diagram. The fatigue limit stress range of notched specimen is predicted using the proposed methodology and compared with a wide range of experimental data available in the literature. Very good agreement is observed between model predictions and experimental observations. Several conclusions can be drawn based on the results in this paper.

- (1) The developed asymptotic solution is effective for application to notched specimen fatigue limit analysis if the SIF with small crack correction is included following the El Haddad model.
- (2) The proposed asymptotic SIF solution is shown to be suitable for both short and long cracks, which indicates that it can be used for future life prediction and crack growth analysis where long crack may exist.
- (3) The fatigue notch factor, which is an empirically fitted parameter in classical fatigue theory, can be theoretically determined by the proposed methodology. The fatigue notch factor is related to notch geometry, specimen geometry and material properties. According to the proposed methodology, the fatigue notch factor is proportional to a non-dimensional parameter $\alpha\sqrt{\left(1 + \frac{d}{a_0} \left\{1 - \exp\left[-\frac{a_0}{d} \left(\frac{K_t^2}{z^2} - 1\right)\right]\right\}\right)}$ for edge notched specimen and $\alpha\beta\sqrt{\left(1 + \frac{2d}{a_0} \left\{1 - \exp\left[-\frac{a_0}{2d} \left(\frac{K_t^2}{z^2} - 1\right)\right]\right\}\right)}$ for a center notched specimen.

This study uses a 2D analysis to illustrate the procedure. Further work is required to extend this procedure to 3D analysis, i.e. surface semi-elliptical crack instead of through crack. Current prediction is for infinite life prediction, and finite life prediction needs to be developed in future study. Only elastic analysis is used in this paper as the material can be assumed to be in the elastic state at the infinite life stage. For finite life prediction, plastic correction considering the effect of both notch and crack is needed for accurate fatigue analysis.

Acknowledgements

The research reported in this paper was supported by funds from the Federal Aviation Administration William J. Hughes Technical Center (Contract No. DTFAC-06-C-00017, Project Manager: Dr. Dy Le). The support is gratefully acknowledged.

References

- [1] Taylor D. Geometrical effects in fatigue: a unifying theoretical model. *Int J Fatigue* 1999;21(5):413–20.
- [2] Taylor D. The theory of critical distances. *Engng Fract Mech* 2008;75(7):1696–705.
- [3] Tovo R, Livieri P. An implicit gradient application to fatigue of complex structures. *Engng Fract Mech* 2008;75(7):1804–14.
- [4] Fleck NA et al. The effect of hole size upon the strength of metallic and polymeric foams. *J Mech Phys Solids* 2001;49(9):2015–30.
- [5] Gomez FJ, Elices M. Fracture of components with V-shaped notches. *Engng Fract Mech* 2003;70(14):1913–27.
- [6] Elices M et al. The cohesive zone model: advantages, limitations and challenges. *Engng Fract Mech* 2002;69(2):137–63.
- [7] Ciavarella M, Meneghetti G. On fatigue limit in the presence of notches: classical vs. recent unified formulations. *Int J Fatigue* 2004;26(3):289–98.
- [8] Bannantine JA, Comer JJ, Hankrock JL. *Fundamentals of metal fatigue analysis*. Upper Saddle River, New Jersey: Prentice Hall; 1990.
- [9] Peterson RE. Notch sensitivity. In: Sines G, Waisman JL, editors. *Metal fatigue*. New York: MacGraw-Hill; 1959. p. 293–306.
- [10] Neuber H. *Theory of notch stresses*. Springer-Verlag, Vienna Springer Publishers; 1958.
- [11] Heywood RE. *Designing against fatigue*. London: Chapman and Hall; 1962.
- [12] Yao W, Xia K, Gu Y. On the fatigue notch factor K_f . *Int J Fatigue* 1995;17(4):245–51.
- [13] Creager M, Paris PC. Elastic field equations for blunt cracks with reference to stress-corrosion cracking. *Int J Fract Mech* 1967;3:247–52.
- [14] Kujawski D. *Fatigue Fract Engng Mater Struct* 1991;14:953–61.
- [15] Jones R et al. Weight functions CTOD and related solutions for cracks at notches. *Engng Failure Anal* 2004;11(1):79–114.
- [16] Newman JC, Raju IS. Stress-intensity factor equations for cracks in three-dimensional finite bodies subjected to tension and bending loads. In: Atluri Satya N, editor. *Computational methods*. Elsevier Science; 1986. p. 312–34.
- [17] Locke WR, Byrne J, Hussey IW. The influence of confined notch plasticity on small fatigue crack growth. *Int J Fatigue* 1995;17(4):287–92.
- [18] Chell GG. *Engng Fract Mech* 1976;8:31.
- [19] Ahmad HY, Clode MP, Yates JR. Prediction of fatigue crack growth in notched members. *Int J Fatigue* 1997;19(10):703–12.
- [20] Dabayeh AA, Berube AJ, Topper TH. An experimental study of the effect of a flaw at a notch root on the fatigue life of cast Al 319. *Int J Fatigue* 1998;20(7):517–30.

- [21] Hammouda MMI, Sallam HEM, Osman HG. Significance of crack tip plasticity to early notch fatigue crack growth. *Int J Fatigue* 2004;26(2):173–82.
- [22] Cameron AD, Smith RA. Upper and lower bounds for the lengths of non-propagating cracks. *Int J Fatigue* 1981;3:9–15.
- [23] Newman JC, Phillips EP, Swain MH. Fatigue-life prediction methodology using small-crack theory. *Int J Fatigue* 1999;21(2):109–19.
- [24] Medved JJ, Breton M, Irving PE. Corrosion pit size distributions and fatigue lives—a study of the EIFS technique for fatigue design in the presence of corrosion. *Int J Fatigue* 2004;26(1):71–80.
- [25] Wenfong L. Short fatigue crack propagation and effect of notch plastic field. *Nucl Engng Design* 2003;220(2):193–200.
- [26] Wu Z, Sun X. Multiple fatigue crack initiation, coalescence and growth in blunt notched specimens. *Engng Fract Mech* 1998;59(3):353–9.
- [27] Kitagawa H, Takahashi S. Applicability of fracture mechanics to vary small cracks or cracks in early stage. In: *Proceedings of 2nd international conference on mechanical behavior of materials*. OH,USA: ASM International; 1976.
- [28] Haddad El, Topper MH, Smith KN. Prediction of nonpropagating cracks. *Engng Fract Mech* 1979;11:573–84.
- [29] Jergéus H. A simple formula for the stress intensity factors of cracks in side notches. *Int J Fract* 1978;14:113–6.
- [30] Härkegård G. An effective stress intensity factor and the determination of the notched fatigue limit. In: Bäcklund J, Blom AF, Beevers CJ, editors. *Fatigue thresholds: fundamentals and engineering applications*. Engineering Materials Advisory Services Ltd.; 1982. p. 867–79.
- [31] Wormsen A, Fjeldstad A, Harkegard G. The application of asymptotic solutions to a semi-elliptical crack at the root of a notch. *Engng Fract Mech* 2006;73(13):1899–912.
- [32] Anderson TL. *Fracture mechanics: fundamentals and applications*. CRC Press; 1995.
- [33] Tada H, Paris PC, Irwin GR. *The stress analysis of cracks handbook*. Del Research; 1985.
- [34] Tada H, Paris PC, Irwin GR. *The stress analysis of cracks handbook*. 2nd ed. Paris Productions Inc.; 1985.
- [35] Nowell D, Dini D, Duó P. Stress analysis of V-notches with and without cracks, with application to foreign object damage. *J Strain Anal Engng Des* 2003;38(5):429–41.
- [36] Atzori B, Lazzarin P, Meneghetti G. Fracture mechanics and notch sensitivity. *Fatigue Fract Engng Mater Struct* 2003;26(3):257–67.
- [37] Ren W, Nicholas T. Notch size effects on high cycle fatigue limit stress of Udimet 720. *Mater Sci Engng A* 2003;357(1-2):141–52.
- [38] Frost NE, March KJ, Pook LP. *Metal fatigue*. Oxford: Oxford University Press; 1974.
- [39] Pilkey WD. *Peterson's stress concentration factors*. 2nd ed. John Wiley and Sons; 1997.
- [40] Benthem JP, Koiter WT. In: Sih GC, editor. *Mechanics of fracture*, vol. 1. Noordhoff International Publishing; 1973. p. 131–78.
- [41] Janssen M, Zuidema J, Wanhill RJH. *Fracture mechanics*. London, New York: Taylor and Francis Routledge; 2004.